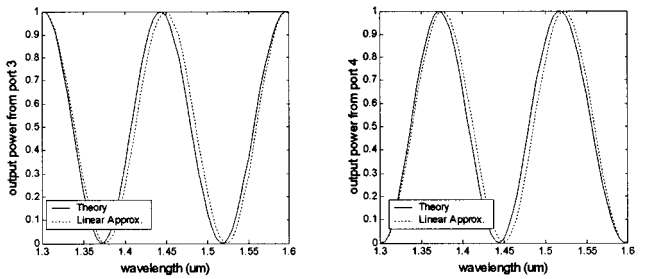

Figure 7 Output power (P_3 and P_4) versus wavelength for a fiber coupler

and

$$P_4 = P_1 \sin^2[(a\lambda + c)z], \tag{11}$$

where $c = -bs$ and z is the coupling length.

Figure 7 shows the output power versus wavelength for a fiber coupler. Solid lines represent the theoretical outputs (assumed to be exact), and the dotted lines are the outputs calculated using the linear approximation. In this example calculation, the coupling length is fixed at 4 cm and the spacing is set at 4 μm. From Figure 7 it is seen that the linear approximation tracks the theoretical result very well. For designing WDM couplers or calculating the output of optical couplers, the simple relationship presented here is easier to use (and often more insightful) than the more precise techniques cited.

REFERENCES

1. D.K. Mynbaev and L.L. Scheiner, Fiber-optic communications technology, Prentice Hall, New Jersey, 2001, pp. 6–25.
2. Y. Kuhara, Y. Fujimura, H. Nakanishi, Y. Iguchi, H. Terauchi, N. Yamabayashi, Y. Ishiguro, and H. Kanamori, Optical WDM transceiver module using wavelength-selective coupler and WDM-PD for optical acess networks, J Lightw Technol 15 (1997), 704–710.
3. A.D. McAulay, Optical guided wave arithmetic, Opt Eng 38 (1999), 468–476.
4. G.E. Keiser, A review of WDM technology and applications, Opt Fiber Technol 5 (1999), 3–39.
5. A.K. Ghatak and K. Thyagarajan, Introduction to fiber optics, Cambridge University Press, New York, 1998, p. 366.
6. R. Tewari and K. Thyagarajan, Analysis of tunable single mode fiber directional couplers using simple and accurate relations, J Lightwave Technol 4 (1986), 386–390.
7. R.G. Hunsperger, Integrated optics: theory and technology, 4th ed., Springer, New York, 1995, pp. 113–119.
8. K. Gerd, Optical fiber communications, 3rd ed., McGraw-Hill, New York, 2000, pp. 390–393.
9. W.B. Jones, Jr., Introduction to optical fiber communication system, Holt, Rinehart, and Winston, Inc., New York, 1988, pp. 71–77.

A SIMPLE FIBER-BRAGG-GRATING SENSOR SYSTEM BASED ON A LINEAR-CAVITY FIBER LASER

Peng-Chun Peng, Hong-Yih Tseng, and Sien Chi
Institute of Electro-Optical Engineering
National Chiao-Tung University
Hsinchu, Taiwan, 300, R.O.C.

Received 13 September 2002

ABSTRACT: *A simple fiber-Bragg-grating (FBG) sensor system based on a linear-cavity fiber laser is proposed and experimentally demonstrated. The lasing wavelength shift resulting from the temperature variation on this sensing element is discriminated by two FBGs. These two FBGs, acting as wavelength discriminators, are used to increase the real-time measurement range for monitoring the temperature variation.* © 2003 Wiley Periodicals, Inc. Microwave Opt Technol Lett 37: 15–17, 2003; Published online in Wiley InterScience (www.interscience.wiley.com). DOI 10.1002/mop.10810

Key words: *fiber sensor; fiber Bragg grating; linear-cavity fiber laser; temperature sensor*

1. INTRODUCTION

The fiber-Bragg-grating (FBG) sensor system has attracted a great deal of interest [1]. By interrogating the Bragg wavelength shift in FBG, an FBG sensor system can measure the temperature variation. To detect such a wavelength shift in FBG, many FBG sensor configurations have been proposed [1–3]. The light source for the simplest FBG sensor configuration is a broadband source, such as an erbium-doped fiber (EDF) pumped by a 980-nm laser diode. After the broadband source is fed into the FBG sensor, the back-reflected light from the FBG provides the sensing information by the reflected wavelength shift. The wavelength shift of this sensing FBG can be interrogated by using an optical spectrum analyzer, a Mach–Zehnder interferometer, and a scanning fiber Fabry–Perot filter. However, the optical power reflected from FBGs is usually weak. This drawback limits the signal-to-noise ratio (SNR) and sensing resolution of the fiber sensor system.

EDF lasers are very important for the applications of fiber communication. We have also proposed a linear-cavity EDF laser array with self-equalized lasing power by using the 980-nm pump reflectors [4]. In this paper, we propose a simple FBG sensor system based on a linear-cavity fiber laser and two FBGs acting as wavelength discriminators. The light source of this FBG sensor system is a linear-cavity fiber laser. One of the cavity mirrors is a fiber loop, and the other is an FBG simultaneously acting as the sensing element. The lasing wavelength shift due to the temperature variation in this sensing element is discriminated by two other FBGs. Because of these two wavelength discriminators and the EDF laser source, we can improve the sensing accuracy for temperature measurement. Moreover, this sensor system can prevent the errors induced by scanning the whole spectrum of the sensing element. Hence, the background noise resulting from such a scanning process can be avoided in our system.

2. EXPERIMENTS AND RESULTS

Figure 1 shows the schematic diagram of the proposed fiber-laser-based FBG sensor system. The EDF laser comprises a fiber-loop mirror, a polarization controller (PC), a fiber-Bragg-grating sensor (FBG1), and a section of EDF pumped by a 980-nm pumping laser. To enhance the capacity for multipoint sensing, we can use the time-division-multiplexing technology by adding a $1 \times N$

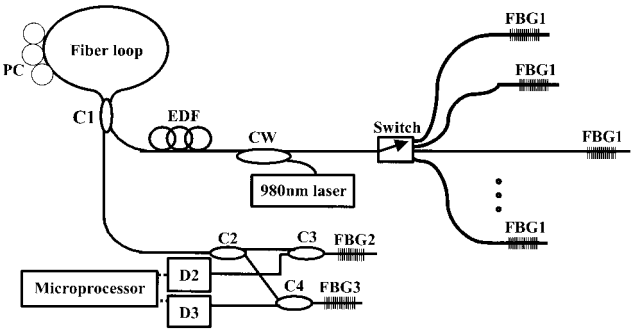

Figure 1 Schematic diagram of the simple FBG sensor system based on a linear-cavity fiber laser

optical switch in this system. The lasing light emerging from the 2×2 coupler ($C1$) travels through a 1×2 coupler ($C2$) and splits into two 1×2 couplers ($C3$ and $C4$) with equal optical power. The backreflected light from FBG2 and FBG3 propagates to the photo detectors ($D2$ and $D3$). The output intensity from each photo detector is then fed into a microprocessor in order to accurately calculate the lasing wavelength by monitoring the reflected power from the two discriminating FBGs.

In this paper, the Bragg wavelength and the peak reflectivity of the sensing FBG1 are 1546.76 nm and 99%, respectively. A 980-nm laser diode, with 130-mW output power, pumps the EDF via a 980/1550-nm wavelength-division-multiplexer coupler (CW). The fiber-loop mirror consists of $C1$ with a coupling ratio of 30:70 and a section of fiber of sufficiently small length to avoid the nonlinear loop effect. Figure 2 shows the output spectrum of the linear-cavity EDF laser. The lasing light travels through $C2$ with a coupling ratio of 50:50 and therefore splits equal power into $C3$ and $C4$. The coupling ratios of $C3$ and $C4$ are both 50:50. The Bragg wavelengths of FBG2 and FBG3 are 1546.88 nm and 1546.94 nm, respectively. Figure 3 shows the normalized reflectivities of FBG2 and FBG3. The relation between the temperature variation and the reflected power from FBG2 and FBG3 is shown in Figure 4, and is measured by an optical power-meter (with minimal detection power -50 dBm). Since the reflected power from FBG2 and FBG3 are nonlinear, the reflected power from FBG2 is used to monitor the temperature variation between 0–25°C with reference to the reflected power from FBG3, and the reflected power from FBG3 is used to monitor the temperature

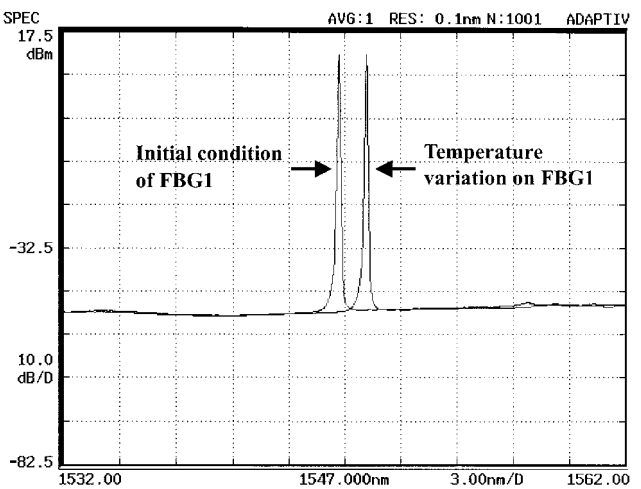

Figure 2 Output spectrum of the linear-cavity EDF laser

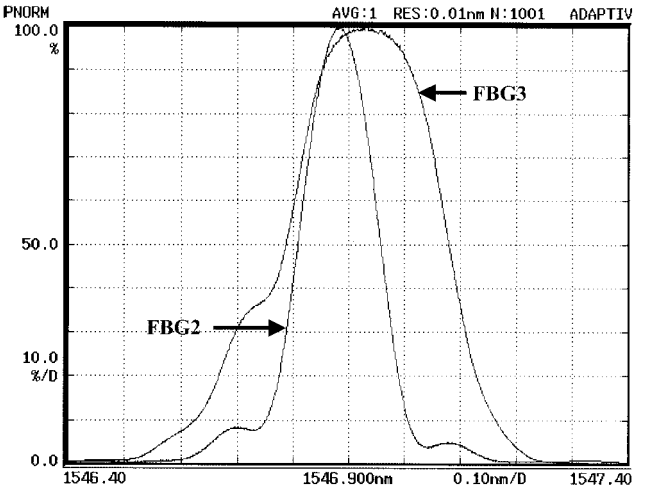

Figure 3 Normalized reflectivities of FBG2 and FBG3

variation between 25–40°C. Consequently, these two discriminating FBGs can increase the measurement range for temperature variation. We can input these relations using a microprocessor to establish a look-up table for real-time measurement of the wavelength shift. Because FBG2 and FBG3 have to discriminate the lasing wavelength, they are arranged in a temperature controller for stable measurement. Moreover, the lasing power of the linear-cavity laser depends on the pumping power, hence we can increase the SNR and the resolution of the whole system by increasing the pumping power of the 980-nm laser diode.

3. CONCLUSION

In summary, we have proposed and experimentally demonstrated a simple FBG sensor system based on a linear-cavity fiber laser and two FBGs acting as wavelength discriminators. These two discriminating FBGs are used to increase the real-time measurement range for monitoring the temperature variation. Such an FBG sensor system can be applied for strain sensing and temperature sensing with high precision.

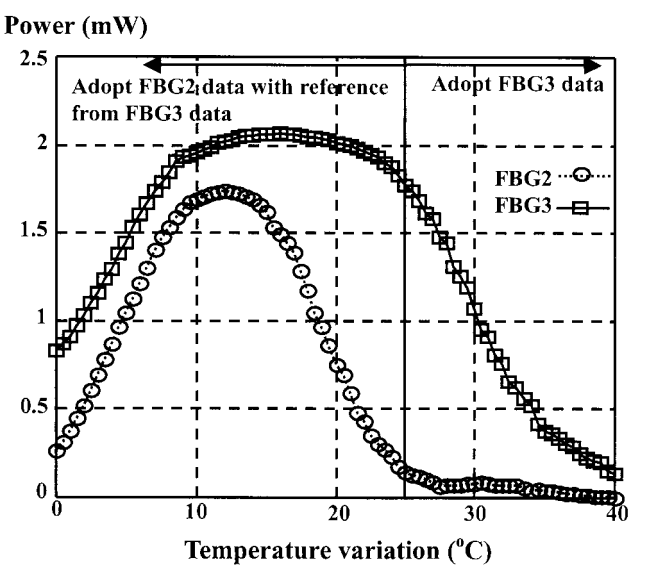

Figure 4 Relation between the temperature variation and the reflected power from FBG2 and FBG3

ACKNOWLEDGMENT

This work was supported by the Academic Excellence Project of Ministry of Education, Taiwan, R. O. C. under Contract 90-E-FA06-1-4-90X023.

REFERENCES

1. A.D. Kersey, M.A. Davis, H.J. Partrick, M. Leblance, K.P. Koo, C.G. Askins, M.A. Putnam, and E.J. Friebele, Fiber grating sensors, J Lightwave Techn 15 (1997), 1442–1463.
2. G.A. Johnson, M.D. Todd, B.L. Althouse, and C.C. Chang, Fiber bragg grating interrogation and multiplexing with a 3 × 3 coupler and scanning filter, J Lightwave Technol 18 (2000), 1101–1105.
3. L. Zhang, Y. Liu, J.A.R. Wiliams, and I. Bennion, Enhanced FBG strain sensing multiplexing capacity using combination of intensity and wavelength dual-coding technique, IEEE Photon Technol Lett 11 (1999), 1638–1641.
4. S.K. Liaw, H.Y. Tseng, and S. Chi, Parallel pump-shared linear cavity laser array using 980-nm pump reflectors or *N* pieces of gain fibers as self-equalizers, IEEE Photon Technol Lett 12 (2000), 19–21.

DIRECTION-OF-ARRIVAL ESTIMATION FOR ULTRA-WIDEBAND EM PULSES WITH AN INTERFEROMETRY

T. Morimoto, A. Hirata, Z. Kawasaki, and T. Shiozawa
Department of Communication Engineering
Osaka University
2-1 Yamada-Oka
Osaka 565-0871, Japan

Received 9 October 2002

ABSTRACT: *In this paper, we present an interferometry for the direction-of-arrival estimation of ultra-wideband electromagnetic waves. The interaction between the antennas composing the interferometer is calculated by using the finite-difference time-domain (FDTD) method, and taken into account in the analysis. We propose a new signal processing scheme for wideband pulses, and demonstrate its effectiveness using a typical wideband pulse.* © 2003 Wiley Periodicals, Inc. Microwave Opt Technol Lett 37: 17–18, 2003; Published online in Wiley InterScience (www.interscience.wiley.com). DOI 10.1002/mop.10811

Key words: *antenna arrays; array signal processing; interferometer; ultra-wideband EM pulse*

INTRODUCTION

Various techniques of direction-of-arrival (DOA) estimation for electromagnetic (EM) waves have been developed in accordance with the spread of wireless communications. As a result, most DOA techniques are applicable only for static monochromatic waves. In other words, less attention is paid to the DOA estimation of ultra-wideband EM waves. Impulsive EM waves from electrical power equipment are a typical example of ultra-wideband EM waves, and their DOA estimations significantly impact EM compatibility. The frequency spectrum of such EM waves is largely dependent on the kind of sources, temperature, humidity, and so forth [1]. Therefore, sufficient intensity of EM power cannot be always obtained by using conventional monochromatic approaches. For a class of EM waves with a wideband spectrum, mutual coupling between antennas would not be negligible at the lower frequency band. In this paper, the concept of conventional interferometry for narrowband is extended for wideband signals.

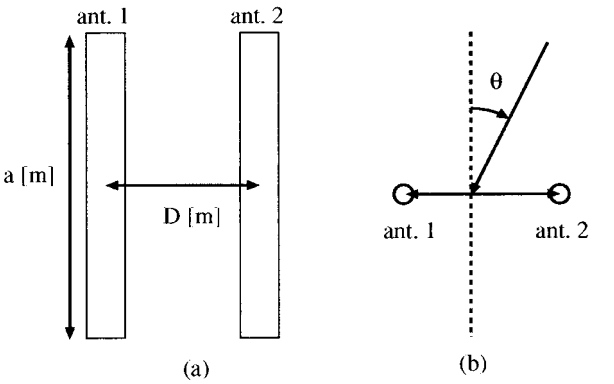

Figure 1 Geometry of the problem: (a) side view; (b) top view. $D = 2.0$ m, $a = 2.7$ m, radius of each antenna is 1.5 mm

First, an interferometer under consideration is analyzed by using the FDTD method to calculate the interaction of antennas. Then, a novel signal processing scheme for wideband pulses is presented with the influence of the antennas' mutual coupling taken into account.

METHODS

We consider two dipole antennas in our DOA estimations (Fig. 1) for simplicity and in order to realize a compact system. Although a dipole antenna is for a narrowband wave, our discussion concentrates on wideband DOA estimations. Therefore, antenna gain is largely dependent on the frequency of EM waves. The idea of using narrowband antennas is validated because the phase difference between antennas is essential in the operation of interferometers.

Mutual impedances of the antenna array are calculated using the FDTD method as a pre-processing step. The detailed procedures can be found in [2]. For an injection of plane wave, we can calculate induced currents at the feeding point of antennas in the time domain. The induced currents are transformed into the frequency domain by fast Fourier transform (FFT). Then, the induced voltages of the antennas for each Fourier component are calculated using the following equations:

$$V_1(f_m) = Z_{11}(f_m)I_1(f_m) + Z_{12}(f_m)I_2(f_m),$$
$$V_2(f_m) = Z_{21}(f_m)I_1(f_m) + Z_{22}(f_m)I_2(f_m), \quad (1)$$

where Z_{11} is the self impedance of antenna 1, and Z_{12} is the mutual impedance between antennas 1 and 2, and $Z_{11} = Z_{22}$ and $Z_{12} = Z_{21}$ (see Fig. 1). The phase difference $\varphi(f_m)$ and estimated DOA $\theta(f_m)$ are determined by the following equations:

$$\varphi(f_m) = [2\pi d \cos \theta(f_m)]/c,$$
$$\theta(f_m) = \cos^{-1}[c\varphi(f_m)/(2\pi f_m d)]. \quad (2)$$

RESULTS

Figure 2 shows the estimated values for the angles of incidence of 45°, 60°, and 75°. It should be noted that these are obtained from the sum of EM pulses modulated by sinusoidal waves. In addition, no noise exists except for that caused by computational error. As seen from this figure, reasonable values for the angles of incidence are obtained. The errors are in the range of 0.5° to 2.5°, although they are dependent on the frequencies of the EM waves. We observe that the errors are mainly caused by the mutual coupling